

Article

Applicability of an Ionising Radiation Measuring System for Real-Time Effective-Dose-Optimised Route Finding Solution during Nuclear Accidents

Attila Zsitnyányi ^{1,*}, János Petrányi ², Jácint Jónás ², Zoltán Garai ², Lajos Kátai-Urbán ^{3,*}, Iván Zádori ¹ and István Kobilka ¹

¹ Doctoral School of Clinical Medicine, University of Pécs Medical School, Szigeti út 12, 7624 Pécs, Hungary; zadori.ivan@kpvk.pte.hu (I.Z.); kobilka.istvan@gmail.com (I.K.)

² Gamma Technical Corporation, Illatos út 11/b, 1097 Budapest, Hungary; petranyi@gammatech.hu (J.P.); jonas.jacint@gammatech.hu (J.J.); garai@gammatech.hu (Z.G.)

³ Institute of Disaster Management, Faculty of Law Enforcement, University of Public Service, Hungária körút 9-11, 1101 Budapest, Hungary

* Correspondence: zsitnyanyi@gammatech.hu (A.Z.); katai.lajos@uni-nke.hu (L.K.-U.)

Abstract: The reduction in the effective dose of evacuated injured persons through contaminated areas of nuclear accidents is an essential emergency services requirement. In this context, there appeared a need to develop a dose-optimised route finding method for firefighting rescue vehicles, which includes the development of a real-time decision support measurement and evaluation system. This determines and visualises the radiation exposure of possible routes in a tested area. The system inside and outside of the vehicle measures the ambient dose equivalent rate, the gamma spectra, and also the airborne radioactive aerosol and iodine levels. The method uses gamma radiation measuring NaI(Tl) scintillation detectors mounted on the outside of the vehicle, to determine the dose rate inside the vehicle using the previously recorded attenuation conversation function, while continuously collecting the air through a filter and using an alpha, beta, and gamma radiation measuring NaI(Tl)+PVT + ZnS(Ag) scintillator to determine the activity concentration in the air, using these measured values to determine the effective dose for all routes and all kinds of vehicles. The energy-dependent shielding effect of the vehicle, the filtering efficiency of the collective protection equipment, and the vehicle's speed and travel time were taken into account. The results were validated by using gamma point sources with different activity and energy levels. The measurement results under real conditions and available real accident data used in our simulations for three different vehicles and pedestrians proved the applicability of the system. During a nuclear accident based on our model calculations, the inhalation of radioactive aerosols causes a dose almost an order of magnitude higher than the external gamma radiation caused by the fallout contamination. The selection of the appropriate vehicle and its route is determined by the spectrum that can be measured at the accident site but especially by the radioactive aerosol concentration in the air that can be measured in the area. In the case of radiation measuring detectors, the shielding effect of the carrier vehicle must be taken into account, especially in the case of heavy shielding vehicles. The method provides an excellent opportunity to reduce the damage to the health of accident victims and first responders during rescue operations.

Keywords: internal radiation exposure; nuclear accident; firefighting rescue vehicle; radiation measurement; dose-optimised route finding



Citation: Zsitnyányi, A.; Petrányi, J.; Jónás, J.; Garai, Z.; Kátai-Urbán, L.; Zádori, I.; Kobilka, I. Applicability of an Ionising Radiation Measuring System for Real-Time Effective-Dose-Optimised Route Finding Solution during Nuclear Accidents. *Fire* **2024**, *7*, 142. <https://doi.org/10.3390/fire7040142>

Academic Editor: Ali Cemal Benim

Received: 19 March 2024

Revised: 5 April 2024

Accepted: 11 April 2024

Published: 16 April 2024



Copyright: © 2024 by the authors. Licensee MDPI, Basel, Switzerland. This article is an open access article distributed under the terms and conditions of the Creative Commons Attribution (CC BY) license (<https://creativecommons.org/licenses/by/4.0/>).

1. Introduction

In the Introduction section, the authors—after the introduction of effective dose radiation measurements systems for route finding rescue procedures—will deal with the analysis of the state of research for route finding methods and its application in the present

study. Finally, they determine the scope of the present research, and then they introduce the research problem and the main research objective of this study.

1.1. Presentation of the Professional Foundations of the Research Problem from the Perspective of Rescue Operations

Protection against the harmful effects of natural and man-made disasters, industrial accidents, and nuclear emergencies requires from the international, regional, and national organisations the introduction of prevention, preparation, and damage control measures [1]. The legal regulatory elements of the international disaster relief and emergency management system can be found among other things in the various policy instruments of the United Nations (UN) and the European Union (EU) organisations. In line with the basic regulations of the International Search and Rescue Advisory Group Guideline [2] and the EU Civil Protection Mechanism (EU CPM) [3]—in addition to the planning, organisation, and management measures of the authorities and operators—the development of a technical instrumentation tool system for the intervention activities is also a necessary requirement [4].

It is necessary to examine the EU regulatory requirements. It can be stated that the EU CPM is a well-coordinated and rapid regional mutual assistance regulation coordinating emergency response activities between member states, for which the essential technical capabilities are provided by national-level organisations. National search and rescue capabilities are significantly necessary to deal with larger-scale emergencies that require the introduction of regional or international cooperation networks and mutual assistance measures [5].

The need to build up national search and rescue technical capabilities in the field of emergency management is supported by several recently published scientific studies, in which the authors examine the disaster management aspects of various emergency situations. Such analyses include, for example, the case of the protection against large-scale forest fires [6], the handling of COVID-19 pandemic events [7], or the preparation for dealing with nuclear emergency situations [8,9]. Of course, the technical intervention capabilities must also be available in case of additional sources of disaster, such as floods, extreme weather conditions, earthquakes, chemical accidents, radiological incidents, and damage to vital critical infrastructure [10]. When planning the involvement of these disaster management technical capabilities, it is an important requirement to integrate the tools and devices—which can be used for all types of danger sources—into the one harmonised and uniform system. Such a technical capability (tools and devices) can be the utilisation of multifunctional firefighting rescue vehicles, when firefighting or rescue forces can intervene in an even shorter time, with greater capacity, with a wider range of abilities, and using more modern and effective technical tools and devices [11].

Due to the above information, firefighting rescue vehicles must also have additional special technical capabilities and features—other than general disaster management and search and rescue abilities—in the case of protection against technogenic emergency situations, like major chemical accidents and also nuclear or radiological emergency accidents and incidents.

The main aim of the present article is the development of firefighting rescue vehicles' special capability, which is used during search and rescue work related to nuclear and radiological emergency situations. In this case, radioactive substances enter into the environment mostly together with the combustion products of major fires [12].

A common feature of the elimination of such an accident event is the presence of dangerous (including radioactive) substances following a major fire or an explosion on the territory of an industrial facility and in the surrounding environment [13]. Emergency response organisations use both installed and mobile systems for monitoring measurements and the evaluation of dangerous substances [14].

The specific technical capabilities of the nuclear accident preparedness activities and the applied tools and devices depend to a significant extent on the effectiveness of the

application of onsite and offsite Chemical, Biological, Radiological and Nuclear (CBRN) emergency response procedures [15]. In the case of a nuclear emergency situation, of course there is also a need for emergency services to rescue injured persons trapped in contaminated industrial areas and facilities [16].

1.2. Introduction of Effective Dose Radiation Measurement Systems for Route Finding Rescue Procedures

During the evacuation process, the amount of the effective dose stands poised for mitigation, contingent upon the judicious selection of the evacuation route, using radiation-shielded vehicles or applying respiratory equipment [17]. Autonomous or remotely controlled Unmanned Ground Vehicles (UGVs) present themselves as a viable arsenal for penetrating these contaminated areas, without imperilling the well-being of any first emergency responders. Many robotic systems have been manufactured and deployed to solve similar scenarios [18,19]. As these machines make their way to their destination in the contaminated area, they have the capability to conduct measurements. This resultant dataset thus accrued serves as a pivotal resource for predicting the effective dose that a person will receive when returning along the same route. If the effective dose calculated for a route exceeds the limits for emergency workers, the UGV should not evacuate the persons on that route or should carry additional shielding and/or respiratory equipment [20].

Engaging in measurements across manifold routes necessitates a considerable temporal outlay, thereby engendering the likelihood of delaying the evacuation procedure [21]. Such an inadvertent delay, however brief, precipitates unnecessary radiation exposure to the person who should be evacuated. A practical way to determine the least contaminated path is to install sensors on various vehicles to measure the ambient dose rate [22]. For vehicles currently equipped with radiation detectors, route finding means driving in the direction in which the lowest dose rate can be measured at that moment. This assumption, however, may lead to a wrong decision for the dose absorbed over the whole path, as it does not take into account the internal radiation exposure at all nor the fact that a shorter path in a direction with an initially higher dose rate may mean an overall lower dose than a longer path, where the vehicle may encounter a higher dose field in the later part of the route.

The existing route finding decision support systems do not take into account that the shielding of the vehicle also depends on the energy of the radiation and therefore incorrectly choose a high-energy-radiation route with a lower dose rate instead of a higher dose rate from low-energy radiation; the new solution takes into account the energy-dependent attenuation factor of the vehicle and recommends a route based on this. In addition, the internal radiation exposure caused by the aerosol in the air and especially iodine must also be taken into account.

Better definition of the content of critical information provision after the initial entry into the radiation-contaminated area will speed up the evacuation process in the shortest possible time.

Should the need arise for re-entry, the autonomous vehicle stands primed to execute further measurements, either across divergent alternative routes or to amend the existing dataset of the same route. Yet, the pinnacle of efficacy resides in applying a larger number of UGVs or drones, orchestrating a synchronous reconnaissance operation across all plausible routes [23]. This method ensures the finding of the optimal exit route in a single engagement.

In the present study, the effective dose was calculated from external exposure measured by ambient dose equivalent rate meters $H^*(10)$ and from internal exposure due to inhalation measured by an online aerosol and iodine monitor [24]. For the prediction of an injured person's effective dose caused by external exposure, the authors used the outside measured value with a Geiger-Müller (GM) tube-based detector and a scintillation-type detector compensated by the shielding effect of the vehicle and multiplied by the time of exposure. The advantage of the GM tube is that it works reliably even with extremely high

gamma radiation (100 Sv/h). The scintillation detector was used for isotope identification and creating a response matrix, which is needed to apply the correct attenuation function for the shielding efficiency calculation. The shielding of the vehicle was characterised with different radioactive sources. The committed effective dose due to inhalation is calculated over a 50-year period after the intake, E50. The E50 cannot be directly measured: it can only be calculated [25]. The online aerosol and iodine monitor sucks in air and measures the alpha, beta, and gamma activity concentration in aerosol and in an activated carbon filter, in particular the radioactive iodine and caesium. The algorithm calculates the intake activity using the occupation time, and the internal effective dose coefficient (dose per intake coefficient) estimates the effective dose to the injured person due to inhalation for each route with and without respiratory protection [26]. The authors used a Phoswich-type scintillation detector to measure alpha, beta, and gamma activity; similar technology was also applied and discussed in Fukushima, Japan [27].

1.3. Analysis of State of Research for Route Finding Methods and Its Application in the Present Study

A large number of publications have been published in connection with route finding procedures and systems. These include, among other things, research related to the control of vehicles [28], sensors [29], and algorithms [30] to be developed in order to avoid obstacles. We can experience a similar situation in the area of route planning using Unmanned Aerial Vehicles (UAVs), which is one of the most important areas in automotive scientific research [31].

For existing and well-functioning route planning solutions found in the literature [32,33], the recommended dose rate should be used as an input parameter. Since these solutions are already available, the goal was not to prepare such a similar route planning solution but also to provide the required dose rate. The existing, modern driving assistance and self-driving solutions are very advanced, even taking into account the inattention of drivers, etc. [34,35]. However, it must be taken into account that during a nuclear accident situation—where these firefighting rescue vehicles are deployed—the behaviour of other vehicles participating in traffic will not be normal. In a normal urban environment without nuclear accident impacts, multisensory route planning solutions use all available data (bus lines, parked cars, internet connection), which results in a significant improvement in the user experience [36,37]. However, in a nuclear accident situation, the availability of these data is uncertain; therefore, robust solutions are necessary.

In the work of Luis Luis M. et al. [38], we can find an excellent summary analysis of the application and development possibilities of mobile radiation detection procedures and devices. A similarly useful study is the review article of Pradeep Kumar A. et. al. [39], which deals with advances in gamma radiation detection systems for emergency radiation monitoring. With regard to the algorithms belonging to the theme of autonomous radiation detection, mapping, and path planning, we can find additional research results created in the area belonging to our current study [40,41]. The evacuation experience following nuclear accidents is also an important question to be analysed, for which we can find many useful publications [42].

In the following, we will monitor the topics related to this research. In 2020, the Gamma Technical Corporation, Budapest, Hungary and the Automotive Research Center of István Széchenyi University, Győr, Hungary conducted research in the field of autonomous systems, including self-driving vehicles and autonomous robots. The main objective of the innovation project was the development of a remote-controlled autonomous vehicle capable of autonomous operation but optionally manned. The goal was to develop and build a basic vehicle that can be used even in difficult terrain conditions and provides protection against physical impacts, which enables multi-purpose application and at the same time ensures the basic conditions of system integration necessary for self-control and provides the possibility to carry replacement superstructures [43].

The present publication is not about the development of sensor systems and algorithms related to autonomous vehicles but about the possible development of a measurement system necessary to solve a special related task.

1.4. Determination of the Research Objectives of the Present Study

The main research objective of the present paper is the development and testing of the applicability of a real-time decision support radiation measurement and evaluation system integrated into an autonomous and radiation-shielded off-road firefighting rescue vehicle which can determine and visualise the radiation exposure of possible rescue routes of territory affected by nuclear accidents or radiological incidents.

The research results of this article should assist in the wider application of UGV tools in nuclear emergency accidents and also response operations in an event requiring the application of CBRN protection forces, tools, devices, and appliances. The system compiled by the authors operates on newly proposed principles and provides higher radiation protection in order to reduce harmful health impacts on accident victims and first responders during emergency response work.

2. Materials and Methods

In this section, the authors—after the introduction of the research design and main steps of the experiments—will briefly deal with the description of the main features of a firefighting rescue vehicle including its radiation protection capabilities, as well as with radiation measuring instruments and radioactive reference sources used for research experiments. Afterwards, the authors will present their measurement and calculation methods and the procedure used for the validation of the experiment's results.

2.1. Introduction of Research Design and Main Steps of the Experiments

In order to investigate the scientific problem introduced in Section 1, the authors have developed a real-time decision support radiation measurement system that determines and visualises the radiation exposure of possible emergency response routes in a given area.

The main steps—in line with the main research objective—of the present research are the following:

1. Creating large-scale homogeneous surface sources with different isotopes.
2. Determination of the energy- and position-dependent radiation shielding efficiency of shielded vehicles to calculate the dose rate inside of the vehicle from any unshielded detector reading.
3. Determination of the G(E) functions for different vehicles.
4. Determination of the external and internal radiation exposure with and without the use of different individual and collective protective equipment.
5. Investigation of the performance of a dose-optimising pathfinding algorithm based on nuclear measurements.
6. Validation of the necessity of the decision support algorithm on constrained paths with known dose rates.

A summary flow diagram of the research design and main steps of the experiments is shown in Figure 1.

We calculated the dose rate from the energy-calibrated gamma spectrum using a spectrum dose conversion operator. This method is known as the G(E) function method [44]. The G(E) function method uses a spectrum dose conversion operator function to calculate the dose rate from the spectrum by multiplying the count rate in each energy channel with the corresponding value of the function and then summing the results.

The measurements were performed with real isotopes and vehicles. Therefore, we did not just carry out computer simulations but reconnaissance with installed isotopes, and the attenuation performance of the vehicles was also measured with real isotopes. Additionally, we used real accident data in simulations of the Chernobyl nuclear accident [45,46].

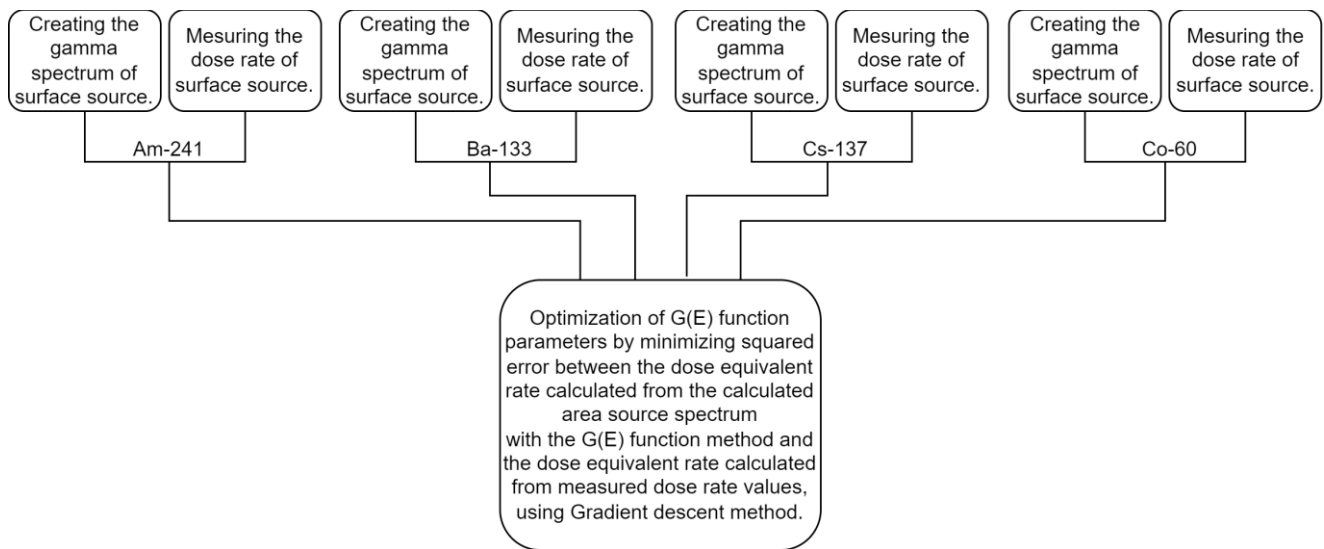


Figure 1. Summary flow chart of research design and the main steps of the experiments. Source: author's own figure.

The vehicles, measuring devices, instrumentation and reference sources, information, technical data, and software used in the performance of the present research tasks were used with the permission of the Gamma Technical Corporation, Budapest, Hungary.

A detailed description of the performance process of the three main experimental steps of this study is given in Figure 1 and in the description materials of the following subsections.

2.2. Description of the Vehicles Used for Research Experiments

During the experiments, we examined the capabilities of three vehicles. The first vehicle is an RDO 3221 KOMONDOR radiation-shielded vehicle developed specifically for nuclear power plant accident prevention and used by the Hungarian Paks Nuclear Power Plant [47]. The second vehicle is an armoured RDO 4336 KOMONDOR heavy all-terrain vehicle used by Hungarian Disaster Management, which is not specifically optimised for radiation protection tasks. The radiation protection parameters of these vehicles were taken into account during a possible escape [48]. The primary application of the third vehicle would be the reconnaissance of the route: the RDO 3927 KOMONDOR vehicle is capable of following the planned route by remote control or in autonomous operation. Of course, such devices are not available everywhere, so we also performed our calculations with the parameters of a traditional vehicle. For these calculations, we used a Citroen Jumper. In a route planning program optimised for nuclear accident prevention, the attenuation factor of the vehicles will have to be a selectable parameter; the route planning algorithm can also take this into account to determine whether the escape can be carried out safely with the given vehicle or, if not, what the expected absorbed dose will be.

Detailed technical information about the KOMONDOR vehicle family used in the present study is provided below:

The RDO 3221 KOMONDOR is a radiation-shielded emergency vehicle, presented in Figure 2, with a radiation detection system, collective protection system containing overpressure and filtration systems, and rescue cabin prepared for quick decontamination, as well as all-wheel-drive and off-road capability. The vehicle can be used as a rescue vehicle during a nuclear accident, for the transport of first response teams or for the evacuation of contaminated persons [47]. This vehicle was used to create a radiation shielding efficiency conversion of the GE function; the spectrum recorded by the unshielded detector was required for the determination of the G(E) function and for the operation of the finished system.



Figure 2. Radiation-shielded emergency vehicle type RDO 3221 RSV KOMONDOR: (a) exterior image and (b) interior image. Source: author's pictures.

The RDO 4336 MPV KOMONDOR is a radiation-shielded multi-purpose heavy-duty firefighting vehicle with different superstructures, presented in Figure 3, with a collective protection system containing overpressure and filtration systems and modular add-on armour, as well as all-wheel-drive and off-road capability. The vehicle can be used as an ambulance vehicle for transporting an injured person on a stretcher [48]. The shielding efficiency conversion of the GE function was adapted and tested with the RDO 4336 MPV vehicle because this system is in operation at the National Directorate General for Disaster Management, Ministry of the Interior, for rescue operations in case of various fire events and nuclear emergencies.



Figure 3. RDO 4336 MPV multi-purpose KOMONDOR with a wide range of interchangeable superstructures: (a) exterior image and (b) interior image. Source: author's picture.

The RDO 3927 KOMONDOR is an autonomous radiation-shielded emergency vehicle, presented in Figure 4, with a radiation detection system, collective protection system for the rescue superstructure part containing overpressure and filtration systems, and modular add-on armour, as well as all-wheel-drive and off-road capability. The vehicle can be used as a reconnaissance vehicle and/or rescue vehicle for transporting contaminated persons. [47]. This vehicle was used in this research to provide on-board measurements. The sensing capability of the vehicle was suitable for measuring radiation with additional spectrometry information. The autonomous operation mode of the vehicle was ideal for investigating the pathfinding concept of this research.



Figure 4. Autonomous vehicle type RDO 3927 KOMONDOR with a rescue (a) and reconnaissance (b) superstructure. Source: author's picture.

2.3. Introduction of the Radiation Measuring Instruments and Radioactive Reference Sources

In this study, a RadGM dose rate transmitter was used to measure the ambient dose rate at a 1 m height. This instrument has a wide measuring range from 50 nSv/h up to 100 Sv/h [49]. To measure the ambient dose rate correctly, the measuring instrument complies with the relevant standard IEC 60846-1 on radiation protection instrumentation [50].

To be able to conduct continuous spectrometry measurements, a scintillation detector called RadNDI was used as well [51]. The RadNDI device combines the capabilities of field and laboratory instruments. This detector has a 2'' × 2'' NaI(Tl) scintillation crystal (18 keV–3 MeV gamma energy), 50 × 1 mm B-10 polyester + Zn/S(Ag) scintillation material (0.025–10 MeV neutron energy). The gamma spectra were evaluated using RadSpect spectrometric evaluation software v. 3.5.7 [52]. A picture of the scintillation detector can be seen in Figure 5. This device automatically provides the measured ambient dose rate, the spectrum, the identified isotopes, and the estimated activity. All measured and calculated data are associated and stored with the actual time and coordinates.



Figure 5. RadNDI scintillation detector [53]. Source: Gamma Technical Corporation, Budapest, Hungary, author's picture.

The third instrument used in this study was the OnRIM Online Radioactive Aerosol and Iodine Monitoring System, which is shown in Figure 6 [53]. This system facilitated the continuous measurement of alpha, beta, and gamma aerosols as well as iodine levels throughout the duration of this study. The air intake point was at the front of the vehicle; prefilter PM10 was used.



Figure 6. OnRIM Online Radioactive Aerosol and Iodine Monitoring System [54]. Source: Gamma Technical Corporation, Budapest, Hungary, author's picture.

The following radioactive reference sources were used for the measurements: ^{241}Am (7.39 GBq, 1.8 MBq), ^{133}Ba (263.7 MBq, 1.5 MBq), ^{137}Cs (784.9 MBq, 1.5 MBq), and ^{60}Co

(120 MBq, 1.1 MBq). They cover a wide photon energy range (59 keV–1.3 MeV). The sources' activity was verified by the Hungarian metrology authority traceable to the Hungarian primary standard for the activity measurement [54].

2.4. Introduction of the Radiation Protection Features of the Firefighting Rescue Vehicle

In order to facilitate the precise determination and comparative assessment of received doses along various exposure pathways, it is essential to evaluate the shielding efficacy of the vehicle, as it permits the calculation of in-vehicle doses based on measurements acquired from an unshielded detector carried by any vehicle type. Similar procedural and methodological scientific information can be found in several benchmark publications related to the subject of the present research [55–57].

The authors' primary objective was to measure the ambient dose rate $H^*(10)$ and spectra with an unshielded detector while also developing a methodology to ascertain the dose rate within a radiation-shielded vehicle. To achieve this goal, the authors devised a $G(E)$ function to calculate the radiation level within the vehicle from spectra obtained by an unshielded or partially shielded detector outside the vehicle. To validate this approach, the authors established a controlled test area featuring known radioactive contaminations [58]. Specifically, the authors opted to employ multiple point-type sealed sources to create a dispersed radioactive contaminated test area, facilitating the evaluation of the proposed methodology [59]. Information on a similar procedure used in international practice can be found in the research publication of Alresheedi M. T. and Elsafi, M. [60].

2.5. Presentation of the Measurement and Calculation Methodology

The measurements were conducted within a 150×150 m flat area devoid of any land objects, as shown in Figure 7. Throughout the measurement process, detectors were positioned centrally within the area, precisely 1 m above the ground level. Point-type sources were systematically placed, measured, and subsequently relocated to new positions for each measurement iteration. Spectra were recorded individually for each source and each source position, ensuring meticulous data collection at every measurement point. During their research, the authors took into account the material elaborated on in several scientific works [61,62]. In all cases, the detector and the vehicle were placed at point 00.

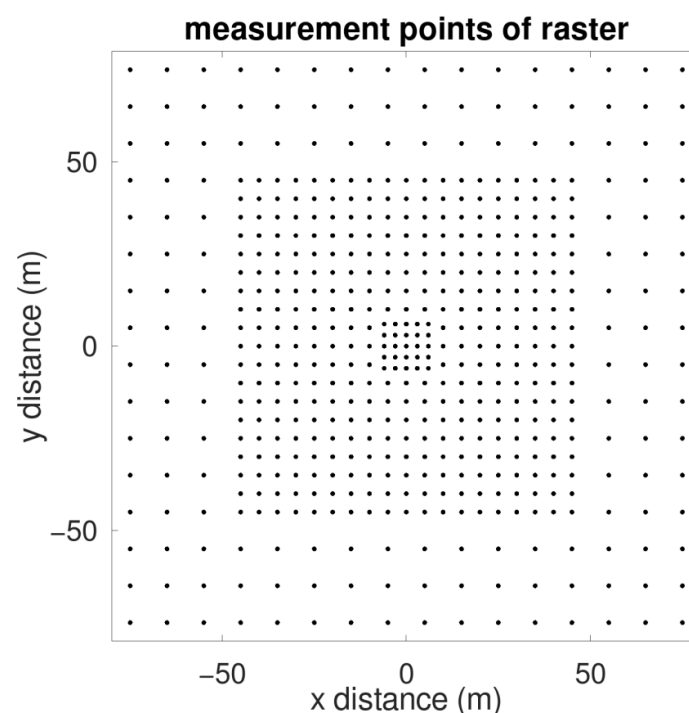


Figure 7. Placement of radiation sources to determine $G(E)$ function. Source: the author's own source.

The measurement points were organised in a grid pattern. Throughout the measurements, the respective point source under examination was positioned precisely at the designated grid point, situated at ground level. It is important to note that for all calculations, we assumed uniform surface radioactivity across the entire measurement area.

Based on our computations, for an infinite homogeneous planar dispersed surface source, the radiation detected at 1 m above the surface within the surrounding area accounts for over 91.6% of the total radiation, in the case of ¹³⁷Cs.

During our measurements, we substituted the dispersed surface source by positioning a point source at various measurement points, where we captured a spectrum at each location. Additionally, we recorded a background spectrum devoid of any point source. More relevant information can be found in the cited scientific publications [63,64].

2.5.1. Calculations for Radiation Measurements

To approximate the spectrum of a dispersed surface source, we aggregated the net measured spectra, weighting each by the area considered to belong to the measured point and the reciprocal of the activity of the source measured at that point, for every energy channel of the spectrum. For the application of a single channel, the formula—prepared by the authors for the purposes of this research—(Formula (1)) is as follows:

$$spt_{tot,j} = \sum_{i=1}^N \frac{S_i}{A_i} \cdot \left(\frac{spt_{src,ij}}{TL_i} - \frac{spt_{bg,j}}{TL_{bg}} \right) \tag{1}$$

where the following abbreviations are included:

- spt_{tot,j}* is the value of the *j*-th channel of the approximated sum spectrum;
- N* is the total number of measurement points;
- S_i* is the area considered to belong to the *i*-th measurement point;
- A_i* is the activity of the point source measured at the *i*-th point;
- spt_{src,i,j}* is the number of counts in the *j*-th channel of the *i*-th measured spectrum, for which the measurement, the live time, is *TL_i*;
- spt_{bg,j}* is the number of counts in the *j*-th channel of the background spectrum;
- TL_{bg}* is the live time of the background spectrum.

Through the weighted summation of 533 spectra for each isotope, we were able to approximate the spectrum of a homogeneous dispersed surface source for these isotopes. The necessity to measure sources with varying activities stemmed from the fact that employing the same source at a distance of approximately 100 m from the detector enabled efficient measurements within a short timeframe, whereas closer distances risked overloading the detector in a matter of meters. Measurement durations ranged from 60 to 600 s.

The energy-dependent shielding efficiency of the various vehicles is shown in Table 1 for ²⁴¹Am, ¹³³Ba, ¹³⁷Cs, and ⁶⁰Co surface sources.

Table 1. Radiation attenuation of different vehicles for different isotopes in the case of homogeneous surface activity concentration. Source: the author’s own work.

	Shielding Efficiency (1-H*(10) _{shielded} /H*(10) _{unshielded}) [1/1]			
	²⁴¹ Am	¹³³ Ba	¹³⁷ Cs	⁶⁰ Co
Pedestrian	0	0	0	0
Normal vehicle	0.9	0.5	0.2	0.1
Vehicle with shielding	1	0.9	0.7	0.6
Vehicle with heavy shielding	1	0.9	0.8	0.7

The squared estimated standard deviation for this value is computed using Formula (2), which was prepared by the authors for the purposes of this research.

$$\Delta spt_{tot,j}^2 = \sum_{i=1}^N \frac{S_i^2}{A_i^2} \cdot \left(\frac{spt_{src,ij}}{TL_i^2} + \frac{spt_{bg,j}}{TL_{bg}^2} \right) \tag{2}$$

The gamma spectrum was obtained using a RadNDI 2'' × 2'' NaI(Tl) scintillation detector positioned at the centre of the test area, precisely 1 m above ground level. Measurements were conducted both without shielding and within the radiation-shielded vehicle, specifically at the position designated for a transferred injured person.

The G(E) function incorporates the distinctive attributes of the entire detector–vehicle system, allowing for the computation of the H*(10) dose rate at identical positions in the presence of dispersed surface sources, such as radioactive fallout. Formula (3) [44] was employed to derive the G(E) function.

$$G(E) = \sum_{K=1}^{KMAX} A(K) \cdot (\log_{10} E)^{(K-M-1)} \quad (3)$$

where the following abbreviations are included:

$KMAX$ is the number of parameters of the G(E) function;

$A(K)$ is the K -th parameter constant of the G(E) function;

E is the photon energy in keV;

M is an offset parameter.

2.5.2. Calculations for the Determination of Protection against Airborne Contamination

The authors determined the internal dose suffered by an injured person from the inhalation of radioactive contamination based on measured activity concentration values by the OnRIM by calculation on the basis of Formula (4), based on a procedure of the International Atomic Energy Agency [24], which was modified by the authors taking into account the filtration efficiency:

$$E_{inh} = \sum_{i=1}^n \bar{C}_{a,i} \cdot CF_{2,i} \cdot T_e \cdot (1 - \eta_{f,i}) \quad (4)$$

where the following abbreviations are included:

E_{inh} is the committed effective dose from the inhalation of radionuclides;

$\bar{C}_{a,i}$ is the activity concentration of radionuclide i in air;

$CF_{2,i}$ is the conversion factor that gives the committed effective dose from the inhalation of contaminated air with unit activity concentration of radionuclide i for unit time;

T_e is the exposure time;

$\eta_{f,i}$ is the filtration efficiency of the air filter for radionuclide i considering the chemical forms that occur during a given accident.

The authors calculated the internal dose of the injured person inside the vehicle by taking into account the filtration efficiency of the air filter [65]. We did not use open isotopes for validation of our calculation. The authors used the measured values and the calculated dose values as an input parameter into the pathfinding algorithm of the UGV. To find the optimal algorithm, we investigated existing data analysis techniques [66].

2.5.3. Summarised Dose Rate Calculation

The summarised dose rate calculation during the operation is shown in Figure 8. In the case of an available vehicle, the program continuously calculates the gamma dose rate suffered inside the vehicle from the outside spectra recorded by the vehicle or UAV. The system also continuously calculates the committed effective dose rate (due to the inhalation) for the selected filter. It is necessary to sum up the gamma dose rate and the inhalation dose rate. The summarised dose rate is calculated for each point of the surveyed route or area. The dose received along the entire path is the integral of the summarised dose rate over time.

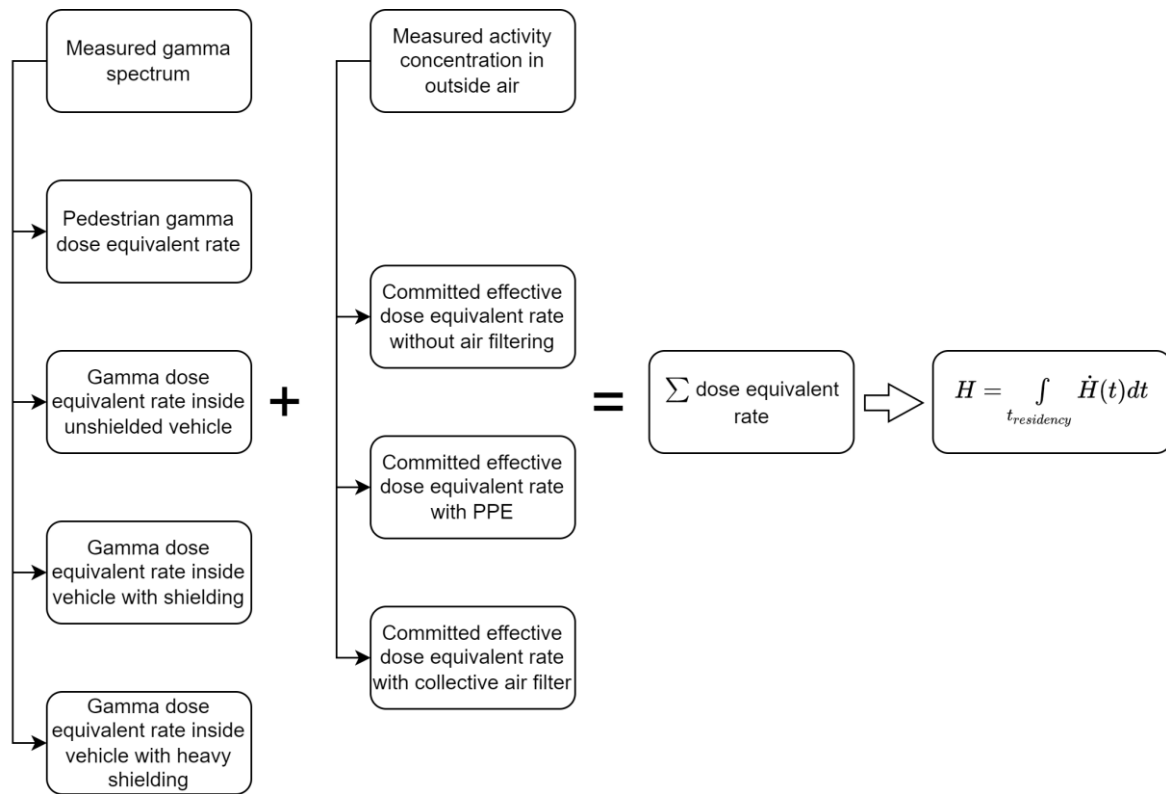


Figure 8. Summarised dose rate calculation during operation. Source: the author’s own source.

2.6. Validation of the Experimental Results

The effectiveness of the method applied was tested in a large building, using a wire ropeway with a motorised automatic detector moving mechanism. The total length of the wire ropeway path was 25 m, with a maximum speed of the detector of 13 km/h and a maximum measurement height of 10 m. The detector with a communication and power module was mounted on the wire ropeway, as in Figure 9.

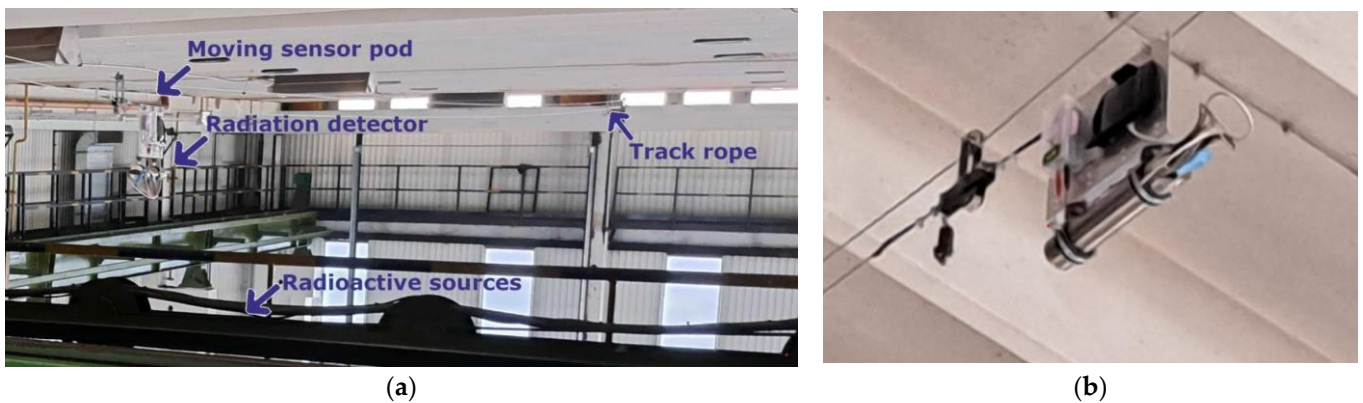


Figure 9. (a) Wire ropeway path with a motorised automatic detector moving mechanism. (b) RadNDI scintillation detector attached to the wire ropeway. Source: the author’s own source.

Three different radioactive sources were placed under the detector to create five different paths, see Figure 10. The detector passed over the sources back and forth 2000 times, covering a path of 100 km. At each end of the track, the detector stopped for 10-10 s (stop for 10 s, pass, stop for 10 s, return). The detector completed one pass cycle in 45 s. The track was about 25 m long, so the detector travelled at an average speed of about 2 m/s when passing from one end of the track to the other.

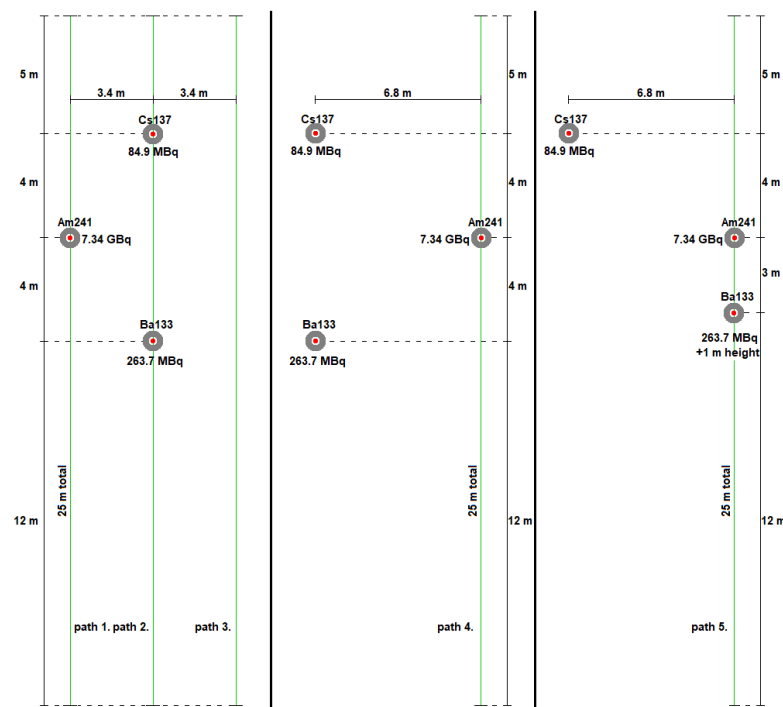


Figure 10. Different measurement paths (marked by green colour) with RadNDI attached to the wire ropeway. Paths 1–5 are marked with a green line in the picture. Source: the author’s own source.

The sources were collimated under the wire ropeway track, but the collimation was conducted with lead bricks, so the angle of the aperture was direction-dependent, and the exact values were not determined. For the first 4 paths, 2000–2000 passes were made while spectra were measured with the detector. Path 5 was part of an additional measurement, where a higher average dose was produced with a low-energy source than when the ^{137}Cs source was on the path. It is certainly more favourable to drive with a shielded vehicle on this path.

Path 4 was also measured for this reason. Path 5 is a good illustration of the fact that the dose is lower on this route when driving a radiation-shielded vehicle than when passing over the ^{137}Cs source, while it is higher when walking.

When calculating the dose from the spectra, it should also be taken into account that the speed is different when walking and when travelling by radiation-shielded vehicle.

Consider the spectra measured for each pathway as if there were a number of different pathway average spectra over a large area, with a large area of radiative material deposited over the background. In this case, the function $G(E)$, defined by the shielding measurements, can be used to calculate the dose rate inside the vehicle from the spectrum measured outside of the vehicle.

An average spectrum and an average dose rate were created for each path. The lowest calculated dose values belong to Path 4, $2.5 \mu\text{Sv}$, and the travel time was the same for all paths, so the algorithm decide to drive on Path 4. The average spectra of all paths can be seen in Figure 11.

The authors validated the measurement method of the scintillation detector with a GM tube-based detector. The measured data showed a high correlation.

The dose values obtained from measurements conducted on the wire ropeway were subjected to validation using the MARCUS constructive simulation software [67]. Within the simulator, five distinct routes were meticulously recorded, virtual models representing the radiation sources employed during the measurements were positioned, and both pedestrian and vehicular movements were simulated along each route. Subsequently, the simulator calculated the dose incurred by both the pedestrian and the vehicle, aligning

closely with the measured results obtained from the wire ropeway course. Figure 12 shows a screenshot captured from the simulation interface.

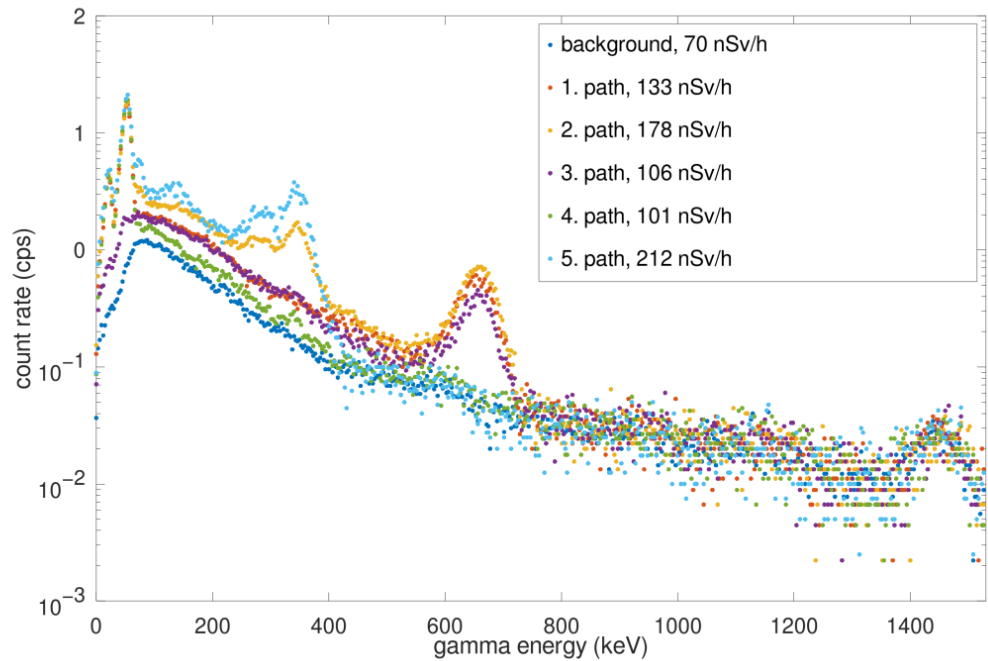


Figure 11. Average spectra measured for different paths. Source: the author’s own source.

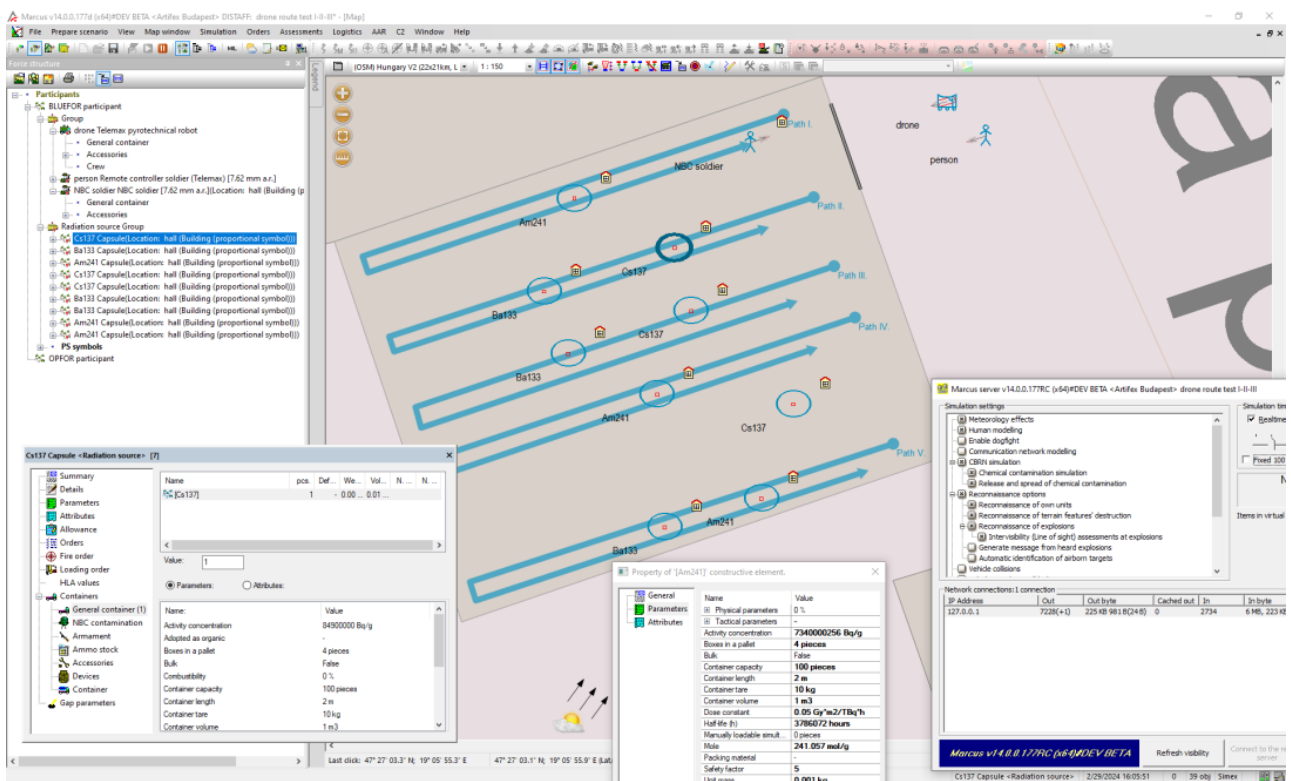


Figure 12. Average spectra measured along different paths using MARCUS simulator software [67].

3. Results and Discussion

This part of this article, based on the calculation and validation experiences, summarises the main research results based on real-time experiences. This section also will deal

with the discussion aspects on the limitation of the applicability of the proposed radiation measurement methodology and on the connection with route finding methods. The novelty of this research and further research possibilities are also discussed in this section.

3.1. Summary and Discussion of Research Measurements, Calculation, and Validation Results

The authors’ research work has primarily covered the following main measurements, calculations, and validation procedures:

1. Measurement of the ambient dose equivalent rate $H^*(10)$ with a RadGM GM tube-based gamma dose rate transmitter.
2. Measurements of the isotopic composition by the RadNDI scintillation detector along with the utilisation of RadSpect spectrometry software.
3. Airborne radioactive aerosols and iodine, causing internal radiation exposure by inhalation, have been measured using the OnRIM alpha, beta, and gamma aerosol and iodine monitor.
4. During the estimation of the effective dose for each route, the dose rate measured inside and outside the vehicle, the shielding effect of the vehicle, the filtering efficiency of the collective protection system, and the speed and travel time of the vehicle were taken into account.
5. The measuring capability of the created test system was validated in a test area using gamma point sources with different activity and energy levels (^{241}Am , ^{133}Ba , ^{137}Cs , and ^{60}Co). The measured values were validated by using the MARCUS constructive simulator.

As a result of the calculation and validation work, several findings were made by the authors, summarised below.

For a detector mounted on a side panel (or the back panel) of the radiation-shielded vehicle, the vehicle attenuates the radiation reaching the detector by 99.999% for ^{241}Am and by 82% for ^{60}Co in the half of the total solid angle which is in the direction of the vehicle and has no attenuation in the other half of the total solid angle; therefore, the average shielding efficiency of the vehicle for the position of the detector for a homogeneous surface source with main gamma energies less than or equal to 1.33 MeV can be considered as 0.5 within an error margin of 20%.

From the dose rate measured by the vehicle-mounted detectors and the dose rate over different paths calculated from the residence time, the optimal path with the lowest dose rate can be selected. It is not necessary to determine the isotopes precisely: the spectrum is enough. However, if a detailed raster dose map with known released isotopes is available in the field, isotope-specific dose conversion coefficients can be used to determine the dose absorbed in the vehicle. If raster gamma spectral results are available for the route travelled or for the whole area, the developed method can be used to determine the optimal route, even for different vehicle approaches. Depending on the dose rate allowed, the user can choose which route and vehicle have a lower calculated dose rate than the dose limit.

The results of dose estimation for all paths can be seen in Table 2.

Table 2. Results of dose estimation for all paths, source: the author’s own work.

Effective Dose for Paths 1–5 [μSv]	Path 1	Path 2	Path 3	Path 4	Path 5
Dose without shielding	3.3	4.5	2.7	2.5	5.3
Dose with shielding	1.2	1.3	1.1	1.0	1.2

We summarised the shielding effect related to external gamma radiation in the case of different scenarios (vehicles), determined from measurements, in Table 1. It can be seen that in the case of a pedestrian there is no shielding for external gamma radiation; therefore, the efficiency of the shielding in this case is 0. The different vehicles shield the gamma radiation originating from the radioactive fallout in the contaminated area to a varying extent. It is important to note, however, that this shielding effect is energy-dependent, so

for lower gamma energy, in the case of an area contaminated with ²⁴¹Am, even a normal vehicle has significant shielding. In the case of ²⁴¹Am, the shielding efficiency of a normal vehicle is 0.9, so it lowers the gamma dose rate originating from radioactive ²⁴¹Am surface contamination by 90%. The radiation-protected vehicle attenuates the radiation originating from the ²⁴¹Am-contaminated surface by several orders of magnitude (>99.999%).

In the case of higher energy gamma emitting radionuclides, it can be stated that a normal vehicle attenuates the radiation to a small extent, less than 10% in the case of ⁶⁰Co; therefore, in the case of surface contamination with higher energy gamma emitting radionuclides, the use of a radiation-protected vehicle instead of a normal vehicle is justified. Furthermore, taking into account dose limits, the use of a vehicle with heavy shielding may be required. During our study, we did not take into account the external dose contribution of radionuclides emitting only alpha or only beta radiation because the external dose contribution of these radionuclides in the case of a nuclear accident would be lower by orders of magnitude than that of gamma emitting radionuclides. It is known that the gamma cross-section is energy-dependent, but the illustration of it is really important. It must be highlighted that a device measuring only the ambient dose equivalent rate (H*(10)) would not provide information about the isotopic composition and the energy of the gamma radiation present. So, the energy-dependent cross-section of gamma radiation is known in vain if previously only dose rate values were typically available for the existing radiation conditions. The computational capacity of detectors and computers connected to them already ensures the availability of gamma spectra of the surveyed area continuously even with a time resolution in seconds.

Because an area contaminated by radionuclides from a nuclear accident was—fortunately—not available to us, we used the values in Table 3 for our dose calculations. We chose the activity concentration values arbitrarily, but we took into account data measured during the Chernobyl accident [45,46]. It can be stated that the activity concentration value measurable in the air after a nuclear power plant accident is extremely high; for ¹³¹I, it is 100 kBq/m³, while for ¹⁴¹Ce, it is 1600 kBq/m³. After the Chernobyl accident, values this high were indeed measurable within a 10 km zone. The need for evacuation is realistic inside the area near the accident. Regarding the surface activity concentrations of the radioactive fallout, it can be stated that these are also abnormally high values, 5000 kBq/m² in the case of ¹³⁷Cs. For the occurrence of these high values, a zone melt or explosion in the reactor zone has to happen for the nuclear decay products to enter the air and fall onto the surface by dry or wet deposition.

Table 3. Radioactive contamination of the area (data similar to those measured after the Chernobyl accident), source: the author’s own work.

Concentration of the Radionuclides in Air [kBq/m ³]				Surface Contamination (Activity Concentration) [kBq/m ²]				
¹³¹ I	¹³⁷ Cs	¹⁴⁴ Ce	¹⁴¹ Ce	¹³⁷ Cs	¹³⁴ Cs	¹⁴⁴ Ce	⁹⁵ Zr	⁹⁵ Nb
100	0.7	9.4	1600	5000	2000	55,500	28,700	53,700

We calculated the different doses suffered during evacuation scenarios by taking into account the radiation protection levels in Table 4. To calculate the shielding efficiency for different scenarios, we first calculated the shielding efficiency of each vehicle for each isotope which is listed with surface contamination in Table 3 and then calculated the weighted average of these values using the activity concentration values in Table 3. In the case of a pedestrian, there is no protection from radiation by shielding and there is no respiratory device protection from radioactive aerosol in the air. The different vehicles have different shielding and air filtering with different efficiency values, given in Table 4. It can be seen that even using Personal Protective Equipment (PPE) where the mask is equipped with an air filter with 90% filtration efficiency significantly decreases the amount

of radionuclides inhaled and therefore the committed dose received. The collective air filter built into vehicles with shielding has a filtration efficiency above 99%.

Table 4. Radiation protection parameters determined by measurements used for dose calculations in the case of homogeneous volume source in air and homogeneous surface source on the surface. Source: the author’s own work.

Scenarios	Filtration Efficiency [%]	Shielding Efficiency [1/1]
Pedestrian	0	0
Pedestrian with PPE	90	0
Normal vehicle with PPE	90	0.33
Vehicle with shielding and collective air filter	99.5	0.75
Vehicle with heavy shielding and collective air filter	99.5	0.82

We summarised the dose rate results calculated for different scenarios in Table 5. It can be seen that in the case of a pedestrian an 11,013 μSv committed effective dose results from the inhalation of radionuclides and a 247 μSv external effective dose results from the radioactive surface fallout during one hour of residence time. It can be stated that inside the supposed contaminated area the inhalation of radionuclides results in a higher total effective dose by at least one order of magnitude than the effective dose received from radioactive surface fallout. Different vehicles attenuate the external dose rate according to their shielding efficiency, but even the vehicle with the heaviest shielding dose not attenuate the external radiation by more than one order of magnitude. A significant decrease, by more than one magnitude, is achieved in the dose received from the inhalation of radionuclides with the use of PPE, and the collective air filter in vehicles decreases this dose even more. We can see in Figure 8 that one has to integrate the momentary value of the dose rate over the total residency time to calculate the dose, so by decreasing the residency time we can decrease the dose received; therefore, the vehicles decrease the dose received during evacuation compared to a pedestrian already due to the speed difference. During our work, we did not take into account the speed of vehicles compared to each other, because even the vehicle with the heaviest shielding is capable of a 90 km/h top speed both on the road and off-road, so if the addition of shielding aimed at reducing the external dose results in a speed decrease due to the extra weight, it may instead increase the dose received during evacuation.

Table 5. Dose rate during different scenarios, source: the author’s own work.

Scenarios	Committed Effective Dose Rate [$\mu\text{Sv/h}$]	External Effective Dose Rate [$\mu\text{Sv/h}$]	Total Effective Dose Rate [$\mu\text{Sv/h}$]
Pedestrian	11,013	247	11,260
Pedestrian with PPE	1101	247	1348
Normal vehicle with PPE	1101	165	1267
Vehicle with shielding and collective air filter	55	62	117
Vehicle with heavy shielding and collective air filter	55	44	99

Using the developed method and the defined modified G(E) functions, the dose rate to the inside of any (pre-measured) vehicle can be calculated. In this way, the optimal route and the type of vehicle can be selected.

A new method was developed that allows route finding based on dose prediction using relatively simple affordable detectors. The spectrum analytical method was more accurate for short measurement times and noisy spectra. The measurement results were stored in a standard file format to share information.

3.2. Discussion on the Application of Route Finding Methods

In connection with the materials in the previous chapters and especially in the literature review of Section 1.3, and in connection with the application difficulties of the route find methodology in Section 3.1, the following discussion topics arose:

1. In a real event, airborne radiation reconnaissance can have two purposes. The detection of radioactive materials or contaminated areas can be used to determine the ideal route for exit. In the other case, it is advisable to check the routes considered passable by the vehicles participating in the evacuation in advance by flying and based on the data measured in this way further decide which is the ideal route.
2. During the authors' previous research, they carried out aerial radiation detection using a helicopter, where they also measured large-scale and point-like radiation sources. However, with the measurement instrument developed on the basis of the experiences at that time, they only carried out measurements using a method simulating flight. The purpose of this was primarily to test the method to find out if it is possible to collect measurement data that can be used for research with this solution.
3. In the experiment in the present study, the authors created measuring arrangements where they tried to simulate a real situation by placing different isotopes in different places. In the future, they also plan to examine additional measurement arrangements, and after that, they will carry out comparisons for those involved in aerial reconnaissance, using the arrangement developed on the basis of experience as a benchmark.
4. The authors' objective was to find answers to what kind of radiation-related data should be taken into account during route planning in the case of the elimination of an event related to radioactive substances. During reconnaissance operations, they can rely on data from radiation measuring sensors placed on air or ground vehicles. In this case, they assume that when planning the aerial reconnaissance route, the vehicle does not run into obstacles or that the device can automatically avoid obstacles.
5. The data from aerial reconnaissance must be taken into account during the planning of the vehicle's route, where values above the predetermined limit appear as an obstacle (the route is impassable), and lower radiation values increase the dose absorbed during the route. The authors have the same approach to reconnaissance with vehicles. The vehicle discovers the originally practicable routes assigned to it and corrects or supplements previously available or unavailable data with accurate data that can be measured by the vehicle; based on the displayed values, the driver can decide where to go or continue even with increasing radiation values, reducing exposure by increasing the speed if that is the only possible route.
6. Avoiding the obstacles that appear is a different specialist task. As described in Section 1.3, the original reconnaissance route will be designed in such a way that it is passable; any obstacles that may appear are basic tasks for companies dealing with the autonomous control of vehicles. In a radiation-related task, "invisible" obstacles or "difficulties" appear as a new factor, and our goal was to measure, process, and display them.

Based on the authors' earlier measurements, it will be an additional research task in a later project to determine how it is appropriate to integrate the data discovered in this way for the research groups developing autonomous controls during route finding and planning.

3.3. Discussion on the Applicability of the Measurement Methodology

An important element of the scientific investigation of emergency response operations carried out in the case of major accidents at nuclear facilities are the firefighting and rescue first intervention procedures and the subsequent evacuation of injured persons from a radiation-contaminated accident scene.

In these operations, the on-site and off-site emergency services (fire brigades) apply firefighting rescue vehicles. Reducing the effective dose received by injured persons during the evacuation process from the vicinity of a nuclear accident site is important from both a

legal and a moral point of view. Pre-existing procedures, well entrenched in practice, exist for the retrospective estimation of the effective dose. The retrospective approach possesses a limitation: it solely influences the treatment regimen of those afflicted, exerting no effect on the reduction in the radiation exposures. Hence, there emerges a pressing need for a method for the determination of the dose-optimised rescue route through contaminated areas.

The authors have created a measurement and evaluation system integrated into an autonomous and radiation-shielded off-road firefighting vehicle, operational without live personnel, that selects a route that causes the least possible risk to the health of persons during the rescue process, by reconnaissance of the possible routes and analysis of the collected data.

Regarding the issue of the limitations of the applicability of the proposed approach, the following main conclusions can be made:

- The shielding effect of the vehicle varies from the type of vehicles.
- The body of the vehicle does not have the same shielding efficiency in all directions.
- The efficiency of the filters changes due to time and depending on the humidity of the air.
- The applied ropeway can be used to create reproducible paths but is limited in the number of sources and the extent of contamination.

3.4. Discussion on Novelty of this Research and Further Research Possibilities

Based on the analysis of the research results of this study, the related literature review of Section 1.3, and the earlier discussion, the main novelties of the research work are as follows:

1. With the use of the presented measurement methodology, the energy-dependent radiation shielding of an arbitrary vehicle can be determined.
2. The vehicle carrying the detectors may shield the detectors in a direction-dependent way. In our case, the shielded vehicle attenuated the radiation received by the detector mounted on the back side of the vehicle by approximately 50% compared to an unshielded detector. During the calibration of vehicle-mounted radiation measuring detectors, one has to take into account the influencing effect of the vehicle on the measured value.
3. To choose the appropriate evacuation vehicle (a vehicle with appropriate shielding), it is necessary to know the energy distribution of the gamma radiation that can be measured in the contaminated area, i.e., its spectrum. With the knowledge of the gamma spectrum, the external dose received by persons to be evacuated may be estimated more precisely.
4. By using the G(E) functions determined in advance for different vehicles, one can estimate the dose the evacuated persons would suffer in the event of an escape with these vehicles.
5. The applied surveying method, the route taken in the contaminated area, and especially the survey of the entire area give the opportunity to choose the optimal route because the route causing the minimum dose can be selected by summing up the available dose rate values.
6. During nuclear power plant accidents, it is not enough to measure the $H^*(10)$ value because after an accident the released radionuclides may cause a committed effective dose higher than the external effective dose in the same residency time by one order of magnitude.
7. If the mass of the shielding of the evacuation vehicle decreases the speed of the vehicle, it may increase the total effective dose received during evacuation.

The authors of this study, after the analysis of their research results, determined the following possible further research objectives:

- By upgrading the measurement system, an improvement in the minimum detectable activity and standard deviation can be achieved.

- The altitude and spectrum correction mechanism with live and measured environmental parameters can make the system more precise and quicker, for example, for airborne radiation monitoring applications.
- To validate the method, on-site tests should be conducted with known contamination levels in the soil and in the air. Establishing such conditions is extremely difficult and dangerous.
- The integration of detectors on UAVs and UGVs is already in progress. In this case, two European projects should be highlighted. These projects are named Chemical, Biological, Radiological and Nuclear Reconnaissance and Surveillance Systems [68] and Chemical, Biological, Radiological and Nuclear Surveillance as a Service (CBRN SaaS) [69].

4. Conclusions

In line with the research results introduced in Section 3 of this article, the following final general conclusions can be drawn up:

1. The authors successfully determined the energy-dependent shielding effectiveness of an autonomous radiation-shielded emergency vehicle, enabling the estimation of dose rates for injured persons inside the vehicle using data obtained from unshielded detectors.
2. By developing an algorithm capable of analysing data collected from various pathways, the authors identified the path with the lowest suffered effective dose, taking into account both external and internal dose estimations. The validation of our results was conducted in a designated test area, demonstrating agreement between measured and simulated results.
3. A potential future endeavour could entail the creation of an application similar to Waze or Google Maps, wherein the recommended path for drivers is based not on prevailing traffic conditions but rather on potential radiation exposure. Furthermore, integrating a drone swarm could enhance the system's capabilities by providing parallel data sources, thereby facilitating more comprehensive and real-time dose assessments.

Author Contributions: Supervision and data curation, I.K. and I.Z.; writing—original draft, A.Z.; formal analysis, J.P.; conceptualisation, J.P.; methodology, A.Z. and J.P.; investigation, A.Z., J.J., and Z.G.; visualisation, A.Z.; project administration, L.K.-U.; writing—review and editing, L.K.-U. All authors have read and agreed to the published version of the manuscript.

Funding: This research received no external funding.

Institutional Review Board Statement: Not applicable.

Informed Consent Statement: Not applicable.

Data Availability Statement: Data are contained within the article.

Conflicts of Interest: The authors declare no conflicts of interest. Authors J.P., J.J. and Z.G. was employed by the company Gamma Technical Corporation. The remaining authors declare that the research was conducted in the absence of any commercial or financial relationships that could be construed as a potential conflict of interest.

References

1. UN Office for Disaster Risk Reduction. Words into Action Guidelines. Implementation Guide for Man-made and Technological Hazards. Available online: <https://www.undrr.org/publication/words-action-guideline-man-made/technological-hazards> (accessed on 8 March 2024).
2. International Search and Rescue Advisory Group. INSARAG Guidelines 2020. Available online: <https://www.insarag.org/methodology/insarag-guidelines/> (accessed on 8 March 2024).
3. EUR-Lex. Decision No 1313/2013/EU of the European Parliament and of the Council of 17 December 2013 on a Union Civil Protection Mechanism. Available online: <https://eur-lex.europa.eu/legal-content/EN/TXT/?uri=CELEX:32013D1313> (accessed on 8 March 2024).
4. European Commission. European Civil Protection and Humanitarian Aid Operation. Available online: https://civil-protection-humanitarian-aid.ec.europa.eu/what/civil-protection_en (accessed on 8 March 2024).

5. Bloem, S.; Cullen, A.C.; Mearns, L.O.; Abatzoglou, J.T. The Role of International Resource Sharing Arrangements in Managing Fire in the Face of Climate Change. *Fire* **2022**, *5*, 88. [CrossRef]
6. Santiago-Gómez, E.; Rodríguez-Rodríguez, C. Building Forest Fires Resilience, the Incorporation of Local Knowledge into Disaster Mitigation Strategies. *Soc. Sci.* **2023**, *12*, 420. [CrossRef]
7. Goniewicz, K.; Khorram-Manesh, A.; Hertelendy, A.J.; Goniewicz, M.; Naylor, K.; Burkle, F.M., Jr. Current Response and Management Decisions of the European Union to the COVID-19 Outbreak: A Review. *Sustainability* **2020**, *12*, 3838. [CrossRef]
8. Dent, R.A. Management of Casualties from Radiation Events. *Eur. Burn J.* **2023**, *4*, 584–595. [CrossRef]
9. Chitikena, H.; Sanfilippo, F.; Ma, S. Robotics in Search and Rescue (SAR) Operations: An Ethical and Design Perspective Framework for Response Phase. *Appl. Sci.* **2023**, *13*, 1800. [CrossRef]
10. Centre for Strategy & Evaluation Services. Evaluation Study of Definitions, Gaps and Costs of Response Capacities for the Union Civil Protection Mechanism. Available online: https://ec.europa.eu/echo/system/files/2020-01/capacities_study_final_report_public.pdf (accessed on 8 March 2024).
11. EUR-Lex. Commission Implementing Decision (EU) 2021/88 of 26 January 2021 amending Implementing Decision (EU) 2019/570 as Regards rescEU Capacities in the Area of Chemical, Biological, Radiological and Nuclear Incidents. Available online: <https://eur-lex.europa.eu/legal-content/EN/TXT/HTML/?uri=CELEX:32021D0088> (accessed on 8 March 2024).
12. Kátai-Urbán, L.; Cimer, Z.; Lublós, É.E. Examination of the Fire Resistance of Construction Materials from Beams in Chemical Warehouses Dealing with Flammable Dangerous Substances. *Fire* **2023**, *6*, 293. [CrossRef]
13. Kátai-Urbán, M.; Bíró, T.; Kátai-Urbán, L.; Varga, F.; Cimer, Z. Identification Methodology for Chemical Warehouses Dealing with Flammable Substances Capable of Causing Firewater Pollution. *Fire* **2023**, *6*, 345. [CrossRef]
14. Cimer, Z.; Vass, G.; Zsitnyányi, A.; Kátai-Urbán, L. Application of Chemical Monitoring and Public Alarm Systems to Reduce Public Vulnerability to Major Accidents Involving Dangerous Substances. *Symmetry* **2021**, *13*, 1528. [CrossRef]
15. Rimpler-Schmid, A.; Trapp, R.; Leonard, S.; Kaunert, C.; Dubucq, Y.; Lefebvre, C.; Mohn, H.; EU Preparedness and Responses to Chemical, Biological, Radiological and Nuclear (CBRN) Threats. European Union. 2021. Available online: [https://centrefrancaisnrbc.fr/mediael/EXPO_STU\(2021\)653645_EN.pdf](https://centrefrancaisnrbc.fr/mediael/EXPO_STU(2021)653645_EN.pdf) (accessed on 8 March 2024).
16. Szabó, B.Á.; Koblka, I.; Zádori, I. Cost dynamics of helicopter emergency services: A Hungarian example. *Heliyon* **2023**, *9*, 14336. [CrossRef]
17. Petrányi, J.; Zsitnyányi, A.; Jónás, J.; Garai, Z.; Kátai-Urbán, L.; Vass, G. Assessing the radiation contamination of large areas using advanced technologies. *Radiat. Prot. Dosim.* **2023**, *199*, 915–921. [CrossRef]
18. Kawatsuma, S.; Fukushima, M.; Okada, T. Emergency response by robots to Fukushima-Daiichi accident: Summary and lessons learned. *Ind. Rob.* **2012**, *39*, 428–435. [CrossRef]
19. Banos, A.; Hayman, J.; Wallace-Smith, T.; Bird, B.; Lennox, B.; Scott, T.B. An assessment of contamination pickup on ground robotic vehicles for nuclear surveying application. *J. Radiol. Prot.* **2021**, *41*, 179–196. [CrossRef]
20. International Atomic Energy Agency (IAEA). Safety Standards for Protecting People and the Environment—Occupational Radiation Protection, IAEA, Vienna. 2018. Available online: https://www-pub.iaea.org/MTCD/Publications/PDF/PUB1785_web.pdf (accessed on 8 March 2024).
21. Rossi, F.; Cosentino, L.; Longhitano, F.; Minutoli, S.; Musico, P.; Osipenko, M.; Poma, G.E.; Ripani, M.; Finocchiaro, P. The Gamma and Neutron Sensor System for Rapid Dose Rate Mapping in the CLEANDEM Project. *Sensors* **2023**, *23*, 4210. [CrossRef]
22. Omega, R.L.; Ishigaki, Y.; Permana, S.; Matsumoto, Y.; Yamamoto, K.; Shozugawa, K.; Hori, M. Low-Cost Sensor Deployment on a Public Minibus in Fukushima Prefecture. *Sensors* **2024**, *24*, 1375. [CrossRef]
23. Xu, H.; Ai, X.; Wang, Y.; Chen, W.; Li, Z.; Guan, X.; Wei, X.; Xie, J.; Chen, Y. Ground Radioactivity Distribution Reconstruction and Dose Rate Estimation Based on Spectrum Deconvolution. *Sensors* **2023**, *23*, 5628. [CrossRef]
24. International Atomic Energy Agency, Generic Procedures for Assessment and Response during a Radiological Emergency, IAEA, Vienna. 2000. Available online: https://www-pub.iaea.org/MTCD/Publications/PDF/te_1162_prn.pdf (accessed on 8 March 2024).
25. Medici, S.; Carbonez, P.; Damet, J.; Bochud, F.; Bailat, C.; Pitzschke, A. Detecting Intake of Radionuclides: In Vivo Screening Measurements with Conventional Radiation Protection Instruments. *Radiat. Meas.* **2019**, *122*, 126–132. [CrossRef]
26. International Atomic Energy Agency, Safety Reports Series n°101: Medical Management of Radiation Injuries, IAEA, Vienna. 2012. Available online: <https://www.iaea.org/publications/12370/medical-management-of-radiation-injuries> (accessed on 8 March 2024).
27. Morishita, Y.; Takasaki, K.; Kitayama, Y.; Tagawa, A.; Shibata, T.; Hoshi, K.; Kaneko, J.; Higuchi, M.H.; Oura, M. A phoswich alpha/beta detector for monitoring in the site of Fukushima Daiichi Nuclear Power Station. *Radiat. Meas.* **2023**, *160*, 106896. [CrossRef]
28. Baras, N.; Dasygenis, M. UGV Coverage Path Planning: An Energy-Efficient Approach through Turn Reduction. *Electronics* **2023**, *12*, 2959. [CrossRef]
29. Lowdon, M.; Martin, P.G.; Hubbard, M.W.J.; Taggart, M.P.; Connor, D.T.; Verbelen, Y.; Sellin, P.J.; Scott, T.B. Evaluation of Scintillator Detection Materials for Application within Airborne Environmental Radiation Monitoring. *Sensors* **2019**, *19*, 3828. [CrossRef]
30. Zhao, Z.; Zhang, Y.; Shi, J.; Long, L.; Lu, Z. Robust Lidar-Inertial Odometry with Ground Condition Perception and Optimization Algorithm for UGV. *Sensors* **2022**, *22*, 7424. [CrossRef]

31. Zhao, L.; Qu, S.; Xu, H.; Wei, Z.; Zhang, C. Energy-efficient trajectory design for secure SWIPT systems assisted by UAV-IRS. *Veh. Commun.* **2024**, *45*, 100725. [CrossRef]
32. Sun, G.; Zhang, Y.; Liao, D.; Yu, H.; Du, X.; Guizani, M. Bus-Trajectory-Based Street-Centric Routing for Message Delivery in Urban Vehicular Ad Hoc Networks. *IEEE Trans. Veh. Technol.* **2018**, *67*, 7550–7563. [CrossRef]
33. Xu, J.; Park, S.H.; Zhang, X.; Hu, J. The Improvement of Road Driving Safety Guided by Visual Inattentive Blindness. *IEEE Trans. Intell. Transp. Syst.* **2022**, *23*, 4972–4981. [CrossRef]
34. Yue, W.; Li, C.; Wang, S.; Xue, N.; Wu, J. Cooperative Incident Management in Mixed Traffic of CAVs and Human-Driven Vehicles. *IEEE Trans. Intell. Transp. Syst.* **2023**, *24*, 12462–12476. [CrossRef]
35. Wang, Y.; Sun, R.; Cheng, Q.; Ochieng, W.Y. Measurement Quality Control Aided Multisensor System for Improved Vehicle Navigation in Urban Areas. *IEEE Trans. Ind. Electron.* **2024**, *71*, 6407–6417. [CrossRef]
36. Sun, R.; Dai, Y.; Cheng, Q. An Adaptive Weighting Strategy for Multisensor Integrated Navigation in Urban Areas. *IEEE Internet Things J.* **2023**, *10*, 12777–12786. [CrossRef]
37. Marques, L.; Vale, A.; Vaz, P. State-of-the-Art Mobile Radiation Detection Systems for Different Scenarios. *Sensors* **2021**, *21*, 1051. [CrossRef] [PubMed]
38. Pradeep Kumar, A.; Shanmugha Sundaram, G.A.; Sharma, B.K.; Venkatesh, S.; Thiruvengadathan, R. Advances in gamma radiation detection systems for emergency radiation monitoring. *Nucl. Eng. Technol.* **2020**, *52*, 2151–2161. [CrossRef]
39. Miyombo Ernest, E.; Liu, Y.; Ayodeji, A. Knowledge-Based Navigation Algorithm for Autonomous Radiation Detection, Mapping and Path Planning. 2024. Available online: <https://ssrn.com/abstract=4681443> (accessed on 8 March 2024).
40. Wu, Z.; Yin, Y.; Liu, J.; Zhang, D.; Chen, J.; Jiang, W. A Novel Path Planning Approach for Mobile Robot in Radioactive Environment Based on Improved Deep Q Network Algorithm. *Symmetry* **2023**, *15*, 2048. [CrossRef]
41. Zhang, D.; Luo, R.; Yin, Y.; Zou, S. Multi-objective path planning for mobile robot in nuclear accident environment based on improved ant colony optimization with modified A. *Nucl. Eng. Technol.* **2023**, *55*, 1838–1854. [CrossRef]
42. Ohba, T.; Tanigawa, K.; Liutsko, L.L. Evacuation after a nuclear accident: Critical reviews of past nuclear accidents and proposal for future planning. *Environ. Int.* **2021**, *148*, 106379. [CrossRef] [PubMed]
43. Defence Industry Association of Hungary, Hungarian Defence Industry 2023. Available online: https://vedelmiipar.hu/downloads/tmp/MVSZ_Almanach_2023_web.pdf (accessed on 4 April 2024).
44. Moriuchi, S. A New Method of Dose Evaluation by Spectrum Dose Conversion Operator and Determination of the Operator, Japan Atomic Energy Research Institute 1971. Available online: https://inis.iaea.org/search/search.aspx?orig_q=RN:3016720 (accessed on 4 April 2024).
45. Drozdovitch, V.; Kryuchkov, V.; Chumak, V.; Kutsen, V.; Golovanov, I.; Bouville, A. Thyroid doses due to Iodine-131 inhalation among Chernobyl cleanup workers. *Radiat. Environ. Biophys.* **2019**, *58*, 183–194. [CrossRef] [PubMed]
46. Garger, E.K. Air concentrations of radionuclides in the vicinity of Chernobyl and the effects of resuspension Ukrainian Agricultural Academy of Sciences, Institute of Radioecology, 252033, Kiev, Tolstoy Street 14, Ukraine. *J. Aerosol Sci.* **1994**, *25*, 745–753. [CrossRef]
47. Zsitnyányi, A. Development of Hungarian Light Armoured Vehicles for Disaster Management and Military Applications. *Hadmérnök* **2022**, *16*, 41–53. [CrossRef]
48. Zsitnyányi, A. KOMONDOR—Könnyű páncélvédett bázisjármű család fejlesztése Magyarországon II. rész. *Haditechnika* **2020**, *54*, 35–42. [CrossRef]
49. Gamma Technical Corporation, Budapest, Hungary. RadGM Gamma Dose Rate Transmitter. 2024. Available online: https://gammatech.hu/?mnuGrp=mnuProducts&module=products&lang=eng&group=sugarzasmero_monitoring&product=radgm (accessed on 8 March 2024).
50. International Electrotechnical Commission. IEC 60846-1 Radiation Protection Instrumentation—Ambient and/or Directional Dose Equivalent (Rate) Meters and/or Monitors for Beta, X and Gamma Radiation—Part 1: Portable Workplace and Environmental Meters and Monitors. 2009. Available online: <https://webstore.iec.ch/publication/3682> (accessed on 8 March 2024).
51. Gamma Technical Corporation, Budapest, Hungary. RadNDI Intelligent Scintillation Detector. 2024. Available online: https://gammatech.hu/?mnuGrp=mnuProducts-mnuProducts_Category&module=products&lang=eng&group=sugarzasmero_spektroszkopia&product=radndi (accessed on 8 March 2024).
52. Gamma Technical Corporation, Budapest, Hungary. RadSpect Software. 2024. Available online: https://gammatech.hu/?mnuGrp=mnuProducts&module=products&lang=eng&group=softwares_gamma&product=radspect (accessed on 8 March 2024).
53. Gamma Technical Corporation, Budapest, Hungary. OnRIM Online Radioactive Aerosol and Iodine Monitoring System. 2024. Available online: https://www.gammatech.hu/index.php?mnuGrp=mnuProducts&module=products&lang=eng&group=kornyezetimonitoring_hordozhato&product=onrim&menupath=kornyezetimonitoring-kornyezetimonitoring_hordozhato (accessed on 8 March 2024).
54. Kessler, C.; Burns, D.; Finta, V. Key Comparison BIPM.RI(I)-K1 of the Air-Kerma Standards of the BFKH, Hungary and the BIPM in ⁶⁰Co Gamma Radiation. Available online: [https://www.bipm.org/documents/20126/44696688/BIPM.RI\(I\)-K1_BFKH_2021.pdf/25b878bd-45c7-5803-f91d-de10b9ecb3e9](https://www.bipm.org/documents/20126/44696688/BIPM.RI(I)-K1_BFKH_2021.pdf/25b878bd-45c7-5803-f91d-de10b9ecb3e9) (accessed on 17 March 2024).
55. Abbas, M.I.; El-Khatib, A.M.; Elsafi, M.; El-Shimy, S.N.; Dib, M.F.; Abdellatif, H.M.; Baharoon, R.; Gouda, M.M. Investigation of Gamma-Ray Shielding Properties of Bismuth Oxide Nanoparticles with a Bentonite–Gypsum Matrix. *Materials* **2023**, *16*, 2056. [CrossRef] [PubMed]

56. Yu, H.; Zhu, G.; Zou, Y.; Yan, R.; Liu, Y.; Kang, X.; Dai, Y. Neutron/Gamma Radial Shielding Design of Main Vessel in a Small Modular Molten Salt Reactor. *J. Nucl. Eng.* **2023**, *4*, 213–227. [[CrossRef](#)]
57. Gouda, M.M.; El-Khatib, A.M.; Abbas, M.I.; Al-Balawi, S.M.; Alabsy, M.T. Gamma Attenuation Features of White Cement Mortars Reinforced by Micro/Nano Bi₂O₃ Particles. *Materials* **2023**, *16*, 1580. [[CrossRef](#)] [[PubMed](#)]
58. Zhang, X.; Efthimiou, G.; Wang, Y.; Huang, M. Comparisons between a new point kernel-based scheme and the infinite plane source assumption method for radiation calculation of deposited airborne radionuclides from nuclear power plants. *J. Environ. Radioact.* **2018**, *184–185*, 32–45. [[CrossRef](#)]
59. Petrányi, J. Development of Radiation Shielded Vehicle and on-board monitoring system in the Service of Emergency Responders. In Proceedings of the 5th European International Radiation Protection Association IRPA Congress, The Hague, The Netherlands, 4–8 June 2018; Volume 5, p. 161. Available online: <https://irpa2018europe.com/wp-content/uploads/2019/05/Book-of-Abstracts-v11.pdf> (accessed on 8 March 2024).
60. Alresheedi, M.T.; Elsafi, M. Effect of Waste Iron Filings (IF) on Radiation Shielding Feature of Polyepoxide Composites. *Crystals* **2023**, *13*, 1168. [[CrossRef](#)]
61. Omori, T.; Kato, S. Verification of an Efficient Monte Carlo Model that Interchanges the Geometric Shapes of Plane Source and Detector in Radiation Transport Calculation. *Jpn. J. Health Phys.* **2020**, *55*, 40–45. [[CrossRef](#)]
62. Namito, Y.; Nakamura, H.; Toyoda, A.; Iijima, K.; Iwase, H.; Ban, S.; Hirayama, H. Transformation of a system consisting of plane isotropic source and unit sphere detector into a system consisting of point isotropic source and plane detector in Monte Carlo radiation transport calculation. *J. Nucl. Sci. Technol.* **2012**, *49*, 167–172. [[CrossRef](#)]
63. Valentin, J. A Report of The International Commission on Radiological Protection. 2005. Available online: <https://pubmed.ncbi.nlm.nih.gov/16164984/> (accessed on 8 March 2024).
64. Gméling, K.; Szilágyi, V.; Harsányi, I.; Szentmiklósi, L. Hungarian Fine-to-Coarse Aggregate, a Possible Constituent of Near-Vessel Structural Concrete of Nuclear Power Plants. *Materials* **2023**, *16*, 3520. [[CrossRef](#)] [[PubMed](#)]
65. Gamma Technical Corporation, Budapest, Hungary. Class-2 Threaded Filter. 2024. Available online: https://gammatech.hu/?mnuGrp=mnuProducts&module=products&lang=eng&group=vedofelszereselek_industrial&product=class2 (accessed on 8 March 2024).
66. Golovko, V.V.; Kamaev, O.; Sun, J. Unveiling Insights: Harnessing the Power of the Most-Frequent-Value Method for Sensor Data Analysis. *Sensors* **2023**, *23*, 8856. [[CrossRef](#)]
67. Artifex Simulation and Training Systems Ltd., Budapest, Hungary. MARCUS Comprehensive constructive simulation. 2024. Available online: <http://artifex.hu/en/marcus> (accessed on 8 March 2024).
68. The European Union. Chemical, Biological, Radiological and Nuclear Reconnaissance and Surveillance System (CBRN RSS). 2020. Available online: https://defence-industry-space.ec.europa.eu/system/files/2021-06/EDIDP2020_factsheet_CBRN_DEWS_CBRN-RSS.pdf (accessed on 8 March 2024).
69. The European Union. Chemical, Biological, Radiological and Nuclear (CBRN) Surveillance as a Service (CBRN SaaS) 2018. Available online: https://www.pesco.europa.eu/wp-content/uploads/2019/05/CELEX_32018D1797_EN_TXT.pdf (accessed on 8 March 2024).

Disclaimer/Publisher’s Note: The statements, opinions and data contained in all publications are solely those of the individual author(s) and contributor(s) and not of MDPI and/or the editor(s). MDPI and/or the editor(s) disclaim responsibility for any injury to people or property resulting from any ideas, methods, instructions or products referred to in the content.